ISSN 0208-7774 TRIBOLOGIA 4/2023 p. 65–77
DOI: 10.5604/01.3001.0054.3945

Paweł SZCZYGIEŁ[*], Krystyna RADOŃ-KOBUS[**], Monika MADEJ[***], Tomasz KOZIOR[****]

TRIBOLOGICAL PROPERTIES OF MED610 MEDICAL MATERIAL USED IN POLYJET MATRIX 3D PRINTING TECHNOLOGY

WŁAŚCIWOŚCI TRIBOLOGICZNE MEDYCZNEGO MATERIAŁU MED610 STOSOWANEGO W TECHNOLOGII DRUKU 3D POLYJET MATRIX

Key words: 3D printing, MED610, PJM, friction, wear, tear.

Abstract: 3D printing is increasingly being used in many industries and in medicine. As a result, new materials are being sought and researched, in particular biocompatible materials. Such materials can be used for medical devices, surgical instruments, and orthopaedic devices, as well as in bone surgery, tissue engineering, prosthetics, regenerative medicine, and the creation of drug delivery systems. This paper presents an analysis of the results of tribological testing of a biocompatible material used in 3D printing technology. The tests were conducted on a TRB^3 tribometer (Anton) in a sphere-disk association. The tests were carried out by making cylindrical specimens with a diameter of 40 mm and a height of 6 mm from the MED610 material using photo-curing liquid polymer resin (PJM) technology. The specimens were fabricated in High Quality mode with a layer thickness of 0.016 mm and with different print directions in the X-Z plane: 0°, 45°, and 90°. The analysis was carried out under technical dry friction conditions and in the presence of saline solution (0.9% NaCl). The tests were performed under fixed test parameters, i.e. speed and loading of the specimens. Ball-disc tests were carried out using balls (counter-specimen) made of different materials with a diameter of 6 mm. Studies have shown that the direction of printing affects tribological wear, due to the anisotropic nature of the 3D printing technology. The lowest average coefficient of friction was obtained for specimens with a print direction of 90°.

Słowa kluczowe: druk 3D, MED610, PJM, tarcie, zużycie.

Streszczenie: Druk 3D znajduje coraz szersze zastosowanie w wielu branżach przemysłowych oraz w medycynie. W związku z tym poszukiwane i poddawane badaniom są nowe materiały, w szczególności materiały biokompatybilne. Materiały takie mogą być stosowane do produkcji sprzętu medycznego, narzędzi chirurgicznych i urządzeń ortopedycznych oraz w chirurgii kostnej, inżynierii tkankowej, protetyce, medycynie regeneracyjnej lub do tworzenia systemów dostarczania leków. W pracy przedstawiono analizę wyników badań tribologicznych biokompatybilnego materiału polimerowego, stosowanego w technologii druku 3D. Testy tarciowe zrealizowano przy użyciu tribometru w skojarzeniu kula–tarcza. Badania przeprowadzono na próbkach w kształcie tarczy o średnicy 40 mm i wysokości 6 mm z materiału MED610 uzyskanego przy użyciu technologii fotoutwardzania ciekłych żywic polimerowych (PJM). Próbki wykonano w trybie wysokiej dokładności (High Quality) z grubością warstwy wynoszącą 0,016 mm oraz z różnymi kierunkami wydruku w płaszczyźnie X-Z: 0°, 45° i 90°. Analizę przeprowadzono w warunkach tarcia technicznie suchego oraz smarowania roztworem soli fizjologicznej (0,9% NaCl). Badania wykonano przy stałych parametrach testu, tj. prędkości i obciążenia próbek. Przeciwpróbkę stanowiły kulki o średnicy 6 mm z poliamidu 6.6 oraz polioksymetylenu (POM). Analiza wyników badań wskazały, iż kierunek druku ma wpływ na zużycie tribologiczne, co wynika z anizotropowej natury technologii druku 3D. Najmniejszy średni współczynnik tarcia uzyskano dla próbek o kierunku wydruku 90°.

[*] ORCID: 0000-0002-3113-3557. Kielce University of Technology, Faculty of Mechatronics and Mechanical Engineering, Tysiąclecia Państwa Polskiego 7 Ave., 25-314 Kielce, Poland.
[**] ORCID: 0000-0003-3959-9113. Kielce University of Technology, Faculty of Mechatronics and Mechanical Engineering, Tysiąclecia Państwa Polskiego 7 Ave., 25-314 Kielce, Poland.
[***] ORCID: 0000-0001-9892-9181. Kielce University of Technology, Faculty of Mechatronics and Mechanical Engineering, Tysiąclecia Państwa Polskiego 7 Ave., 25-314 Kielce, Poland.
[****] ORCID: 0000-0002-8922-4187. Kielce University of Technology, Faculty of Mechatronics and Mechanical Engineering, Tysiąclecia Państwa Polskiego 7 Ave., 25-314 Kielce, Poland.

INTRODUCTION

The fourth industrial revolution (Industry 4.0) has embraced many modern manufacturing technologies, 3D printing in particular **[L. 1]**. By means of refining known and developing new 3D printing methods and materials, additive technologies have appeared in the main industry areas: aerospace, automotive, food, medical, construction, textiles, and electronics **[L. 2]**. For the purpose of medical applications, 3D printing has become a focus of research as well as an enabling tool. The analysis of the available literature points towards applications of the 3D printing technology in: implantology **[L. 3, 4],** prosthetics **[L. 5,6],** orthopaedics **[L. 7],** drug delivery systems **[L. 8]**, and transplantology **[L. 9, 10]**. The photo-curing technology of liquid polymer resins used in this study – PJM (PolyJet Matrix) – is used in various areas of medicine as they are made of materials allowing for contact with the skin and oral cavities,: dentistry **[L. 11],** radiotherapy **[L. 12],** bone scaffolding **[L. 13]** or in the manufacture of medical equipment [**L. 14**].

The development of new biomedical materials used for biomedical purposes in additive manufacturing technologies, considering their anisotropic nature, requires the study of their properties in a variety of printing directions, due to the fact that the models are structured in layers. The commonly occurring phenomenon of friction relates to nearly all components manufactured by 3D printing technology during their use; therefore, tribological testing is an extremely important aspect of the research [**L. 15, 16**]. The study of surface topography plays a key role when analysing wear mechanisms; therefore, it is important to have a proper methodology based on a clear objective and test programme [**L. 17**].

3D printing technologies for medical applications also use metallic materials [**L. 18, 19**]. Methods for modifying the surface layer with anti-wear properties operating in biotribological systems are already known [**L. 20–22**]. Promising directions for future research include the modification of the surface layer of printed components made of metallic materials using anti-wear coatings.

The research presented in this article aims to evaluate the tribological properties of a medical-grade material known under the trade name MED610. The paper also evaluates the hardness and surface wettability of printed specimens using the PolyJet Matrix technology. Additive manufacturing technologies have rarely been the subject of tribological research. That fact is evidenced by the low number of scientific publications covering that aspect, in particular the use of such materials for medical applications. Therefore, this article fills this research gap.

MATERIALS AND METHODS

MED610 (Stratasys Corp, Minnesota, Minneapolis) is a medical material approved for permanent skin contact and limited mucosal contact (up to 24 hours). The manufacturer states that the material was developed for medical and dental applications [**L. 23**]. This material meets normative requirements in terms of: irritation and hypersensitivity type IV [**L. 24**]**,** cytotoxicity [**L. 25**]**,** genotoxicity [**L. 26**], and chemical characteristics [**L. 27**]. **Table 1** shows the chemical composition of the material [**L. 28**], while **Table 2** lists the selected material properties in accordance with relevant standards [**L. 28**].

The test specimens were printed using SUP705 support material. The resin turns into a gel during the polymerisation process and is easily removed with a water wash. **Table 3** shows the chemical composition of the support material.

The PJM (PolyJet Matrix) method of photo-curing liquid polymer resins in 3D printing requires the application of droplets of liquid resin on the printer's work bench at the exact location of the cross-section of the model being constructed. Subsequently, UV irradiation of the object initiates

Table 1. Chemical composition of the MED610 material [L. 28]
Tabela 1. Skład chemiczny materiału MED610 [**L. 28**]

Component	Isobornyl acrylate	Acrylic monomer	Urethane acrylate	Acrylic monomer	Epoxy acrylate	Acrylate oligomer	Photoinitiator
Weight %	15–30	15–30	10–30	5–10; 10–15	5–10; 10–15	5–10; 10–15	0.1–1; 1–2

Table 2. Material properties of MED610 [L. 28]
Tabela 2. Właściwości materiału MED610 [**L. 28**]

Property	Scale/Standard	Value
Tensile strength	ASTM D-638-03	50–65 MPa
Elongation at rupture	ASTM D-638-05	10–25 %
Young's modulus	ASTM D-638-04	2000–3000 MPa
Flexural strength	ASTM D-790-03	75–110 MPa
Flexural modulus	ASTM D-790-04	2200–3200 MPa
Poisson's ratio*	ASTM D638-10	0.41
Deflection temperature	ASTM D-648-06	45–50°C
Water absorption	ASTM D-570-98 24HR	1.1–1.5%
Shore (Rockwell) hardness	D scale (M)	83–85 D (73–76 M)
Biocompatibility	EN ISO 10993-1:2017	Skin contact – permanent Contact with mucous membranes – up to 24 hours

* The value of the Poisson's ratio was emailed by Stratasys at the authors' request.

Table 3. Chemical composition of the Support SUP705 material [L. 29]
Tabela 3. Skład chemiczny materiału Support SUP705 [**L. 29**]

Component	Polyethylene glycol	Propylene glycol	Glycerol	2-hydroxyethyl acrylate	A proprietary agent
Weight %	10–30	10–30	10–30	3–10	0.1–0.3

the polymerisation process and transition from the liquid to the solid state. This process is repeated layer after layer until the finished 3D model is obtained. Components manufactured using additive technologies are characterised by a pronounced anisotropy. This means that the properties of the printed models are dependent on the direction of printing [**L. 30**].

The specimens used for the purpose of the study were made using the PJM technology on an Objet 350 machine manufactured by Connex (currently Stratasys). The models were made in High Quality print mode, using the smallest possible layer thickness of 0.016 mm.

The specimens are discs with a diameter of 40 mm and a height of 6 mm, manufactured of the MED610 material through PJM 3D printing technology. The specimens were made with three preset print directions (angles) – PD (Print direction): 0^o, 45^o, and 90^o (**Figure 1**). A key element included the surface preparation of the specimens, which were sanded using a Pace Technologies grinding-polishing machine with sandpaper of varying grain granulation: 120, 240, and 600 µm. The specimens obtained had a surface roughness of S_a = 0.8 µm, the parameter was measured using a Leica DCM 8 confocal microscope. The obtained value is the arithmetic mean of the measurements of the three specimen types (0°, 45°, 90°). Each specimen was measured five times. Based on the series of measurements, the standard deviation (SD) from the specimen was calculated, amounting to SD = 0.06.

a) b)

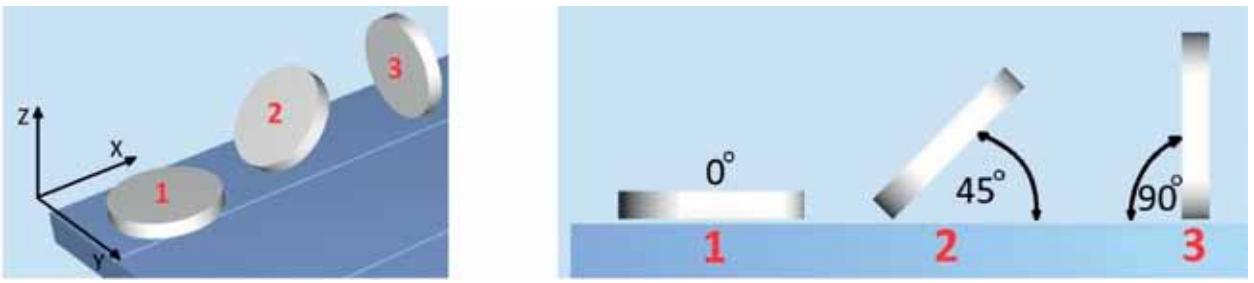

Fig. 1. Positioning of the specimens on the 3D printer virtual worktable: (a) arrangement of specimens, (b) print directions used: 1 – 0° printout, 2 – 45° printout, 3 – 90° printout

Rys. 1. Orientacja próbek na wirtualnym stole roboczym drukarki 3D: (a) ułożenie próbek, (b) zastosowane kierunki wydruku: 1 – wydruk 0°, 2 – wydruk 45°, 3 – wydruk 90°

The counter-specimens were 6 mm diameter spheres made of polymer plastics in the form of unmodified POM (polyoxymethylene) and PA 6.6 (polyamide) with the trade names Delrin and Nylon 6.6, respectively. Lightweight spheres made of POM display good mechanical properties, corrosion resistance, wear resistance, and abrasion resistance (**Table 4**). POM shows resistance to alkaline compounds, neutral and weak acids, seawater, petroleum products, mineral oils and greases, inorganic salt solutions, aliphatic, aromatic hydrocarbons and chlorine, low-grade alcohols, and ether. However, this material is not resistant to strong acids (hydrochloric, phosphoric, nitric, and sulphuric), mineral acids, chlorides and alkalis **[L. 31]**. Given these properties, POM is used in the food, chemical, electronic as well as pharmaceutical industries for applications ranging from spray mixers, lightweight safety valves, bearings, special pumps and valves to fluid control equipment and medical instruments.

The second type of a sphere material was semicrystalline thermoplastic polyamide 6.6. It is characterised by low weight and high resistance to corrosion and tribological wear (**Table 5**). Its additional properties include self-lubrication, good ductility, strength, and electrical insulating properties. The beads are insoluble in dilute mineral acids and in most organic acids. In addition, they are resistant to alkalis, petroleum products, lubricants, inorganic salt solutions, low-grade alcohols, motor oils, transmission fluids, methanol, ketones, and

Table 4. Properties of Delrin (POM) [L. 31]
Tabela 4. Właściwości Delrin (POM) **[L. 31]**

Property	Symbol	Unit of Measure	Type	Notes	Values
Density	δ	g/cm^3	Physical	Room temp.	1.40
Water absorption	Aw	%	Physical	24h	0.30
Young's modulus	E	MPa	Mechanical	-	2800
Friction coefficient	μ	-	Mechanical	Room temp.	0.28
Hardness	-	Shore D	Mechanical	-	80–90
Compressive yield strength	-	MPa	Mechanical	-	30–120
Coefficient of linear thermal expansion	α	10^{-6}/°C	Thermal	(ΔT=0-100°C)	93
Thermal conductivity	λ	W/(m · K)	Thermal	Room temp.	0.27
Service temperature	-	°C	Thermal	-	-4085
Volume resistivity	ρ	Ω · m	Electric	-	> 10^{13}
Relative magnetic permeability	μ_m	-	Magnetic	Diamagnetic	< ~1

Table 5. Properties of Nylon 6.6 (PA 6.6) [L. 32]
Tabela 5. Właściwości Nylon 6.6 (PA 6.6) **[L. 32]**

Property	Symbol	Unit of Measure	Type	Notes	Values
Density	δ	g/cm^3	Physical	Room temp.	1.11
Water absorption	Aw	%	Physical	24h	2.10
Young's modulus	E	MPa	Mechanical	-	2500
Friction coefficient	μ	-	Mechanical	Room temp.	0.25
Hardness	-	Shore D	Mechanical	-	75–85
Compressive yield strength	-	MPa	Mechanical	-	86–103
Coefficient of linear thermal expansion	α	10^{-6}/°C	Thermal	(ΔT=0-100°C)	87.50
Thermal conductivity	λ	W/(m · K)	Thermal	Room temp.	0.25
Service temperature	-	°C	Thermal	-	-3080
Volume resistivity	ρ	Ω · m	Electric	-	> 10^{13}
Relative magnetic permeability	μ_m	-	Magnetic	Diamagnetic	< ~1

esters. However, this material is not resistant to strong acids and alkalis **[L. 32]**. These spheres are used in dedicated valves, bearings, flow meters, hand grips as well as in the medical industry.

Specimens and counter-specimens were used to carry out tribological tests in a sphere-disc association. Tests were performed under technically dry friction conditions, including saline lubrication (0.9% NaCl). The present study used specimens which varied in terms of the direction of printing, the counter-specimens used and the tribological test conditions. Three different printing directions of the specimens, the counter-specimens made of two materials, and two types of friction (dry technical friction or with a lubricant) brought forth 12 different tribological tests. Each was repeated three times.

Test methods

Surface topography before and after tribological testing was obtained with a Leica DCM 8 interferometric mode confocal microscope through a 20x magnification lens in a confocal mode. The following parameters were generated for surface topography measurements: S_a (arithmetic mean height), S_p (maximum peak height), S_v (maximum valley depth), S_z (maximum height of surface), S_{sk} (asymmetry), and S_{ku} (kurtosis).

The tribological tests were carried out on a TRB^3 tribometer (Anton Paar) in rotary motion. The tests were carried out under conditions of technically dry friction as well as friction under lubrication with saline solution. The tests were repeated three times for each specimen. Their parameters are presented in **Table 6**.

Table 6. Tribological test parameters
Tabela 6. Parametry testu tribologicznego

Load [N]	Velocity [m/s]	Friction radius [mm]	Distance [m]	Temperature [°C]	Humidity [%]
10	0.1	12	1,000	25± 2	45±5

The Attension Theta Flex optical tensiometer was used to determine the wettability of the surface of the specimens depending on the printing directions. Wetting angle measurement consisted in precisely depositing a droplet of the measuring liquid (distilled water, diiodomethane and saline) on the surface of the specimen and performing immediate measurements. The droplets were deposited randomly on the surface of the specimen. Mean wetting angles with standard deviations were calculated through five measurements. The hardness of the specimens for the different printing directions was tested using a Hildebrand Shore D hardness tester. The measurements were made in accordance with the ISO 868 standard.

RESULTS AND ANALYSIS

Surface topography measurements

Table 7 contains the measured parameters describing the shape (topography) of the surface of the specimens made of MED610 depending on the direction of printing, and **Figure 2** shows examples of isometric views and surface profiles.

The analysis of the surface topography measurements of the specimens taken in the three print directions shows that the arithmetic mean height is the lowest for the 45° specimens (0.77µm) and the highest for the 90° specimens (0.88µm). For the other parameters, the 45° specimen also ranked the lowest, while the highest values were registered for the 0° specimen, for instance the maximum peak height – 11.72 µm. Nevertheless, the values of the parameters describing the surface topography of the specimens did not differ significantly from one another.

Wettability measurements

Figure 3 shows views of distilled water droplets, **Figure 4** shows views of diiodomethane droplets, and **Figure 5** shows views of saline droplets on specimen surfaces made in the three print directions. The measurement was carried out on 9 specimens prior to tribological testing. **Figure 6** shows the values of the average wetting angles for the MED610 surface, which were calculated from five measurements.

Table 7. Measured specimen roughness parameters
Tabela 7. Zmierzone parametry chropowatości próbek

Print direction	S_{sk}	S_{ku}	S_p [µm]	S_v [µm]	S_z [µm]	S_a [µm]
0°	-0.80	5.09	11.72	16.67	28.39	0.81
45°	-0.37	3.49	5.97	5.44	11.41	0.77
90°	-0.44	3.38	7.10	11.39	18.49	0.88

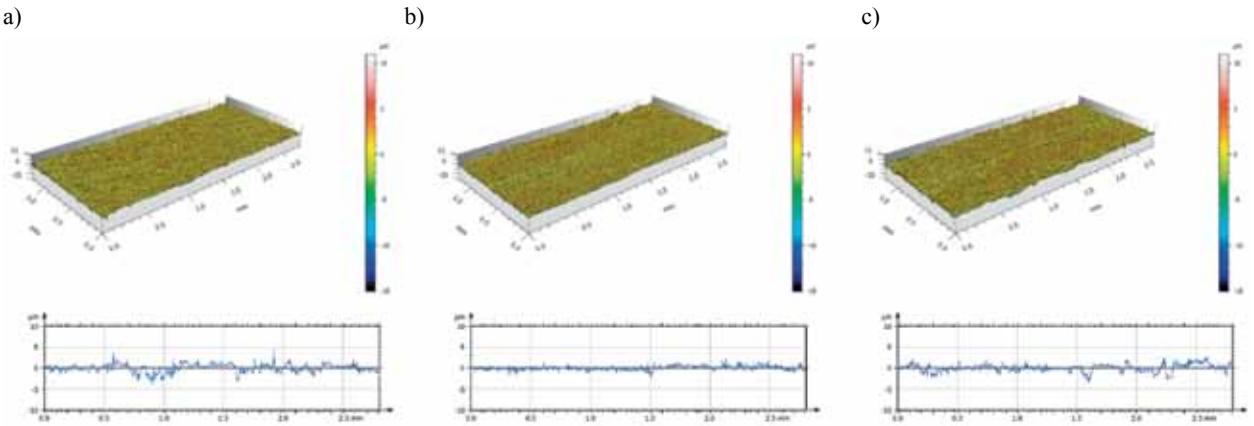

Fig. 2. The isometric view and surface profiles of the MED610 depending on the printing direction (a) 0°, (b) 45°, (c) 90°
Rys. 2. Widok izometryczny oraz profile powierzchni MED610 w zależności od kierunku wydruku (a) 0°, (b) 45°, (c) 90°

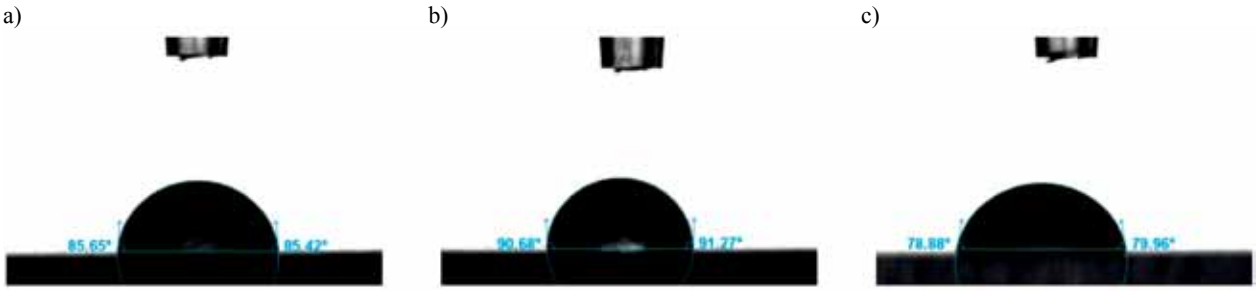

Fig. 3. View of the distilled water droplet on the MED610 surface for the print direction (a) 0°, (b) 45°, (c) 90°
Rys. 3. Widok kropli wody destylowanej na powierzchni MED610 dla kierunku wydruku (a) 0°, (b) 45°, (c) 90

Fig. 4. View of the diiodomethane droplet on the MED610 surface for the print direction (a) 0°, (b) 45°, (c) 90°
Rys. 4. Widok kropli dijodometanu na powierzchni MED610 dla kierunku wydruku (a) 0°, (b) 45°, (c) 90°

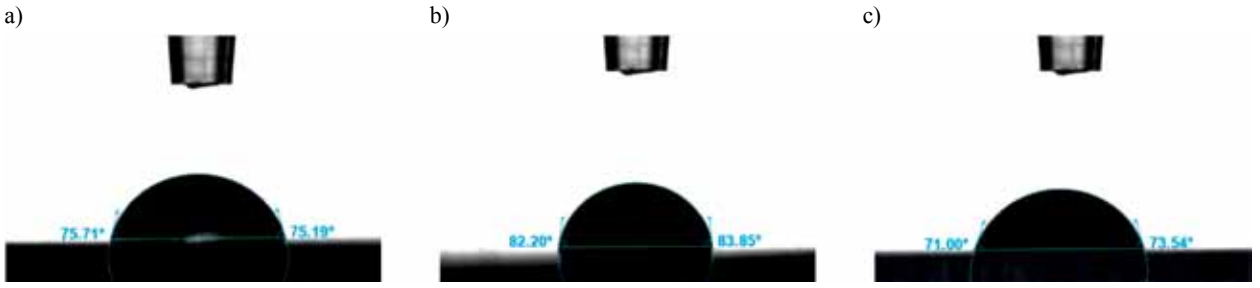

Fig. 5. View of the saline droplet on the MED610 surface for the print direction (a) 0°, (b) 45°, (c) 90°
Rys. 5. Widok kropli soli fizjologicznej na powierzchni MED610 dla kierunku wydruku (a) 0°, (b) 45°, (c) 90°

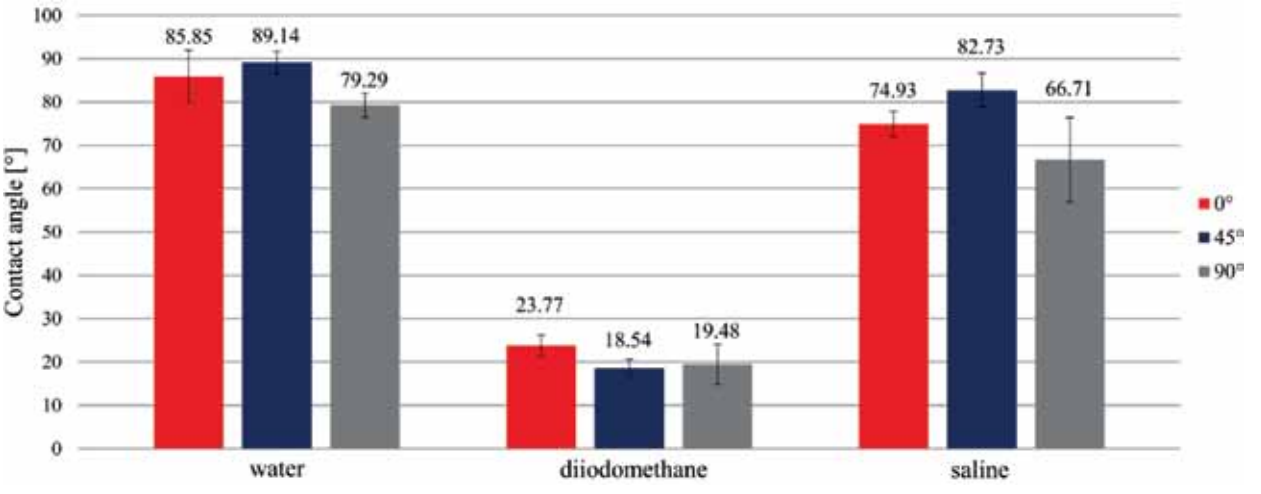

Fig. 6. Average wetting angle values for the MED610 surface
Rys. 6. Średnie wartości kątów zwilżania dla powierzchni MED610

The smallest wetting angle for distilled water was obtained for a specimen made with a print direction of 90°, and the largest for a specimen with a print direction of 45°. This demonstrates the hydrophobic nature of the surface of the specimen with the 45° direction, in contrast to the specimen with the 90° and 0° print directions, which are characterised by hydrophilicity. The smallest diiodomethane wetting angle was obtained for a specimen with a print direction of 45°, while the largest for 0°. The smallest saline surface wetting angle was obtained for the 90° specimen and the largest for the 45° specimen.

When analysing the average values for the wetting angle determined with distilled water, the lowest value was obtained for specimens with a print direction of 90° – 72.29°, and the highest for specimens with a print direction of 45° – 89.14°. The value obtained for specimens with a print direction of 45° oscillates within the limits of the hydrophobic surface. In the case of diiodomethane, the highest values of the average wetting angles were obtained for the surface of specimens with a print direction of 0° – 23.77°, and the lowest for specimens with a print direction of 45° – 18.54° (although the differences between the 45° and 90° specimens are insignificant). A saline surface wettability test showed the highest wettability for the 45° print direction of 82.73° and the lowest for the 90° specimen surface of 66.71°.

Hardness measurement

Table 8 shows the Shore D hardness values, depending on the direction of printing.

Table 8. Shore D hardness averages according to the direction of printing

Tabela 8. Wartości średnie twardości w skali Shore'a D w zależności od kierunku wydruku

No.	1 (PD – 0°)	2 (PD – 45°)	3 (PD – 90°)
1	83	82	82
2	82	81	82
3	83	83	82
4	83	84	81
5	83	83	83
Mean	82.8	82.6	82

Hardness measurements were carried out using specimens made in accordance with the accepted three printing directions. Average values were obtained through five measurements of hardness. The differences between the average hardness values of each specimen type are lower than 1 percent. Such a low variety indicates that the direction of printing has no significant effect on the surface hardness of the surface. The specimens on which the hardness measurements were taken were not reused for the remaining tests.

Tribological tests

Figure 7 shows the values of the average friction coefficients for the MED610 specimens, made in the three print directions, after tribological tests with a PA 6.6 sphere and POM sphere, respectively, under a load of 10 N.

In the case of the PA 6.6 counter-specimen, the highest average coefficient of friction during

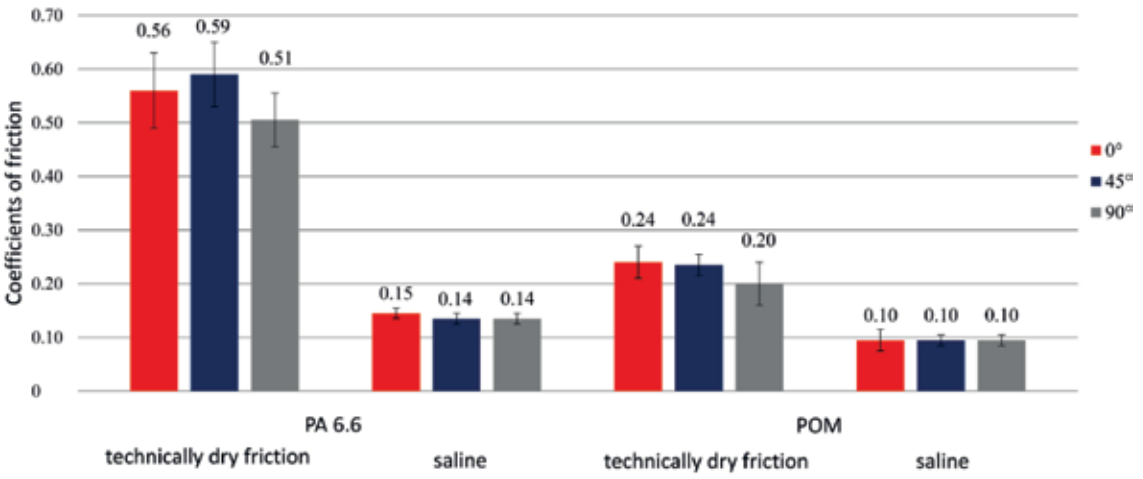

Fig. 7. Average values of friction coefficients for specimens after tribological tests with a load of 10 N with a counter-specimen made of PA 6.6 and POM

Rys. 7. Wartości średnie współczynników tarcia dla próbek po testach tribologicznych przy obciążeniu 10 N z przeciwpróbką wykonaną z materiału PA 6.6 oraz POM

technically dry friction was obtained for the 45° specimens – 0.59, and the lowest for the 90° specimens – 0.51. The coefficient of friction for the 90° specimen is approximately 13% lower than in case of the 45° specimen. During friction involving the use of saline, the mean values of the friction coefficients for all directions tested oscillated at 0.14. In the case of the PA 6.6 counter-specimens, the highest average coefficient during technically dry friction was obtained for the 45° specimens – 0.24, and the lowest for the 90° specimens – 0.20. The coefficient of friction for the 90° specimen is approximately 17% lower than for the 0° and 45° specimens. During friction involving the use of saline, the mean values of the friction coefficients for all printing directions oscillated at 0.10.

Figure 8 shows isometric views and surface profiles depending on the printing direction (0°, 45°, 90°), after technical dry friction and with saline lubrication using a sphere made of PA 6.6 material.

Figures 8a, 8b and **8c** show isometric views and surface profiles of the specimens for 0°, 45°, 90° print directions, after technically dry friction, and **Figures 8d, 8e** and **8f** after friction under saline solution lubrication. Small traces of abrasion were observed after friction with saline, which cannot be determined due to the roughness of the surface of the specimens.

Figure 9 depicts the isometric views and surface profiles depending on the printing direction (0°, 45°, 90°) after technical dry friction and with

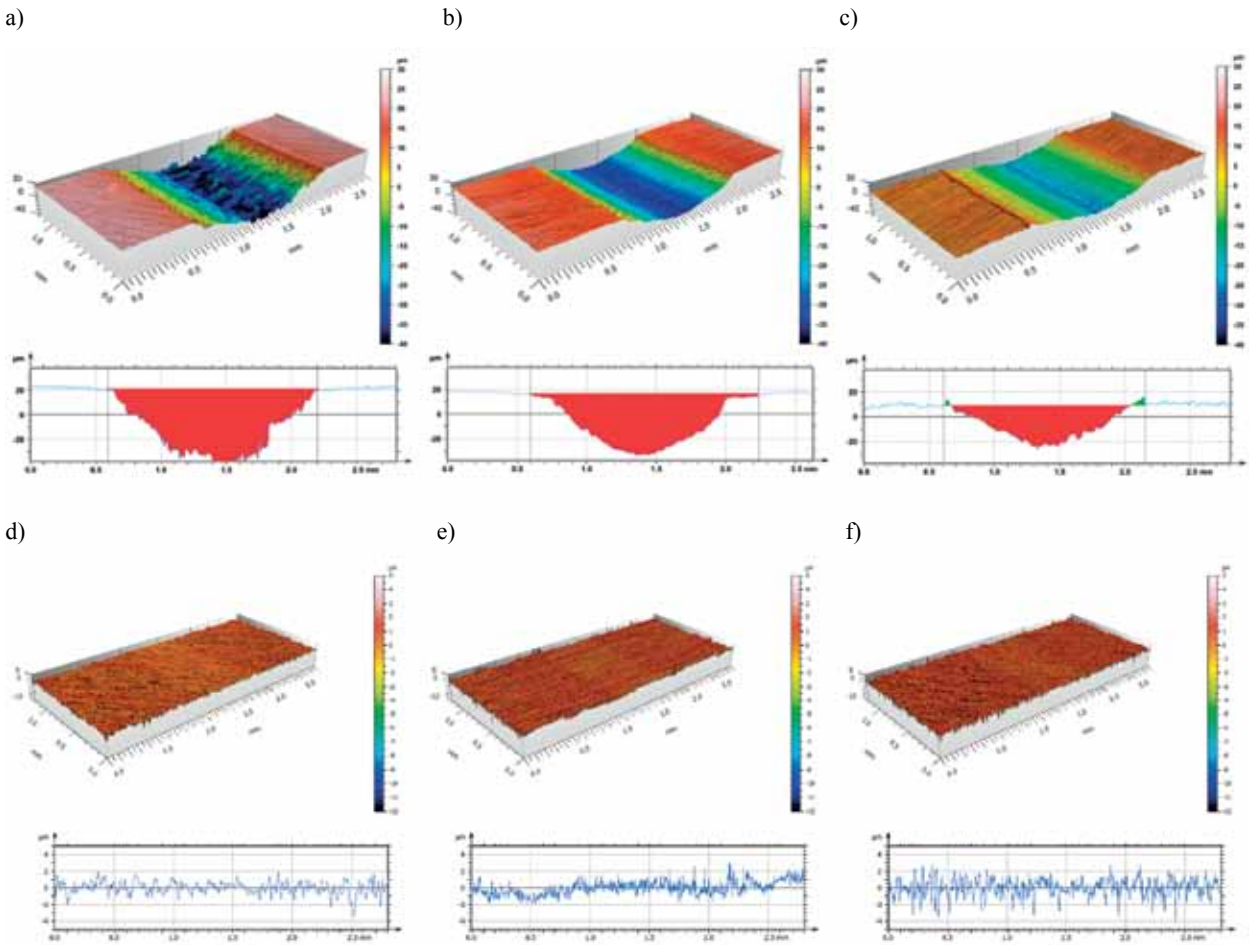

Fig. 8. Isometric views and surface profiles of specimens made of MED610 depending on the direction of printing at 10N load after tribological tests with a PA 6.6 sphere: (a) dry-technical friction printing direction 0°, (b) dry-technical friction printing direction 45°, (c) dry-technical friction printing direction 90°, (d) saline friction printing direction 0°, (e) saline friction printing direction 45°, (f) saline friction printing direction 90°

Rys. 8. Widoki izometryczne oraz profile powierzchni próbek wykonanych z MED610 w zależności od kierunku wydruku przy obciążeniu 10 N po testach tribologicznych z kulką PA 6.6: (a) tarcie technicznie suche – kierunek wydruku 0°, (b) tarcie technicznie suche – kierunek wydruku 45°, (c) tarcie technicznie suche – kierunek wydruku 90°, (d) tarcie z użyciem soli fizjologicznej – kierunek wydruku 0°, (e) tarcie z użyciem soli fizjologicznej – kierunek wydruku 45°, (f) tarcie z użyciem soli fizjologicznej – kierunek wydruku 90°

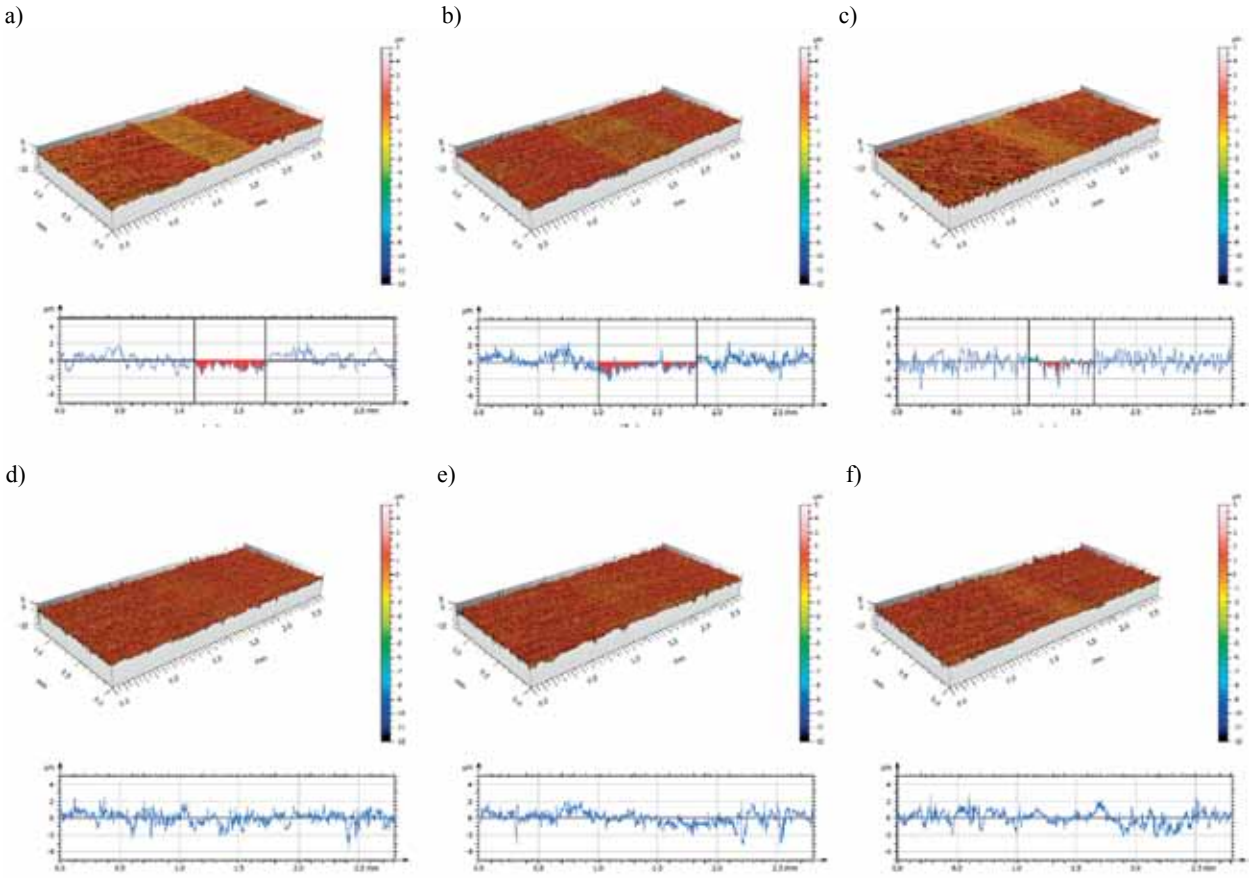

Fig. 9. Isometric views and surface profiles of specimens made of MED610 depending on the direction of printing at a load of 10N after tribological tests with a POM sphere: (a) dry-technical friction printing direction 0°, (b) dry-technical friction printing direction 45°, (c) dry-technical friction printing direction 90°, (d) saline friction printing direction 0°, (e) saline friction printing direction 45°, (f) saline friction printing direction 90°

Rys. 9. Widoki izometryczne oraz profile powierzchni próbek wykonanych z MED610 w zależności od kierunku wydruku przy obciążeniu 10N po testach tribologicznych z kulką POM: (a) tarcie technicznie suche – kierunek wydruku 0°, (b) tarcie technicznie suche – kierunek wydruku 45°, (c) tarcie technicznie suche – kierunek wydruku 90°, (d) tarcie z użyciem soli fizjologicznej – kierunek wydruku 0°, (e) tarcie z użyciem soli fizjologicznej – kierunek wydruku 45°, (f) tarcie z użyciem soli fizjologicznej – kierunek wydruku 90°

saline lubrication using a sphere made of the PA 6.6 material. **Table 9** shows the indicators of abrasion marks on the MED610 surface after the tribological tests.

Figures 9a, 9b and **9c** show isometric views and surface profiles of the specimens for 0°, 45°, 90° print directions after dry friction, and **Figures 9d, 9e** and **9f** – after saline friction. As in the case of the tests carried out with the sphere made of the PA 6.6 material, small traces of abrasion were observed after the application of the saline lubricant.

During tests with counter-specimens made of the PA 6.6 material without lubricant, the highest maximum wear depth was recorded for the 0° specimen at 69.58 µm and the lowest for the 90° specimen at 35.62 µm. The largest wear area was also recorded for the 0° specimen – 60753 µm^2, while the smallest for the 90° specimen –

Table 9. Indices of abrasion marks on the MED610 surface after tribological tests with a load of 10 N

Tabela 9. Wskaźniki śladów wytarcia na powierzchni MED610 po testach tribologicznych z obciążeniem 10 N

Specimen designation (Technically dry friction)	Maximum depth [µm]	Wear area [µm^2]
PD 0° – PA 6.6	69.58	60753
PD 45° – PA 6.6	50.88	45386
PD 90° – PA 6.6	35.62	27543
PD 0° – POM	2.39	529.75
PD 45° – POM	2.38	526.50
PD 90° – POM	4.30	280.75

27543 μm^2. The wear depth for the 90° specimen is approximately 49% lower than for the 0° specimen, and the wear area is approximately 55% lower for the 90° specimen than for the 0° specimen. In the case of the application of a lubricant (saline), no trace of abrasion was observed and, therefore, the depth and area of abrasion were not determined. This was due to the high surface roughness of the test specimens.

Tests carried out using POM material counter-specimens showed that the highest maximum wear depth was recorded for the 90° – 4.30 μm and the lowest for the 45° specimen – 2.38 μm. The largest wear area was recorded for the 0° – 529.75 μm^2 and the smallest for the 90° specimen – 280.75 μm^2. The wear depth for the 45° specimen is approximately 45% lower than for the 90° specimen, and the wear area is approximately 47% lower for the 90° specimen than for the 0° specimen. During the tests carried out with the lubricant, as in the case of the counter-specimens made of PA 6.6, it was not possible to determine the depth and area of wear for the tests carried out.

The analysis of the results shows leads to the conclusion that the direction of the print on the work bench of the 3D printer impacts the surface shaped by operation. Specimens made with a preset print direction of 90° had the smallest wear area, both when using a PA 6.6 and POM material counter-specimen. In this case, the force resulting from the load was applied parallel to the technologically shaped layers of the specimen model. When testing the 0° specimen, when the force resulting from the loading was directed perpendicular to the technologically made layers, the results were unfavourable and the surface was characterised by a significant area of abrasion, a difference that is particularly evident when using counter-specimens made of the PA 6.6 material.

CONCLUSIONS

The analysis of the results of the medical MED610 material used in 3D printing allows the following conclusions:

- the direction of printing does not significantly affect the wettability and hardness of the surface;
- during tests under technical dry friction conditions with both POM and PA 6.6 counter-specimens, the lowest average coefficient of friction was obtained for specimens at a print direction of 90°;
- when a saline lubricant was used, lower coefficients of friction were recorded, and the determined average values did not differ according to the direction of printing of the specimens;
- the exceptionally high reduction in the friction coefficient after the application of a lubricant in the test with a sphere made of PA 6.6 results from the water absorption of this material,
- during tests under technically dry friction conditions carried out using a counter-specimen made of the PA 6.6 material, the largest wear area was recorded for specimens with a 0° printing direction, and the smallest for specimens with a 90° printing direction;
- in the case of tests under technically dry friction conditions using a POM counter-specimen, the largest wear area was recorded for specimens with a 0° printing direction, and the smallest for those with a 90° printing direction;
- the direction of printing has a direct impact on tribological wear; and
- 90° specimens whose process layers were aligned parallel to the applied load were characterised by the lowest average coefficient of friction and the smallest area of rubbing for technically dry friction.

ACKNOWLEDGEMENTS

This research was partially funded by the National Science Center of Poland under the Miniatura 4, grant number 2020/04/X/ST5/00057 entitled: Analysis of polymer composites produced by 3D printing and electrospinning technologies in the applications of filtering devices.

REFERENCES

1. Jandyal A., Chaturvedi I., Wazir I., Raina A., Ul Haq M.I.: 3D printing – A review of processes, materials and applications in industry 4.0. Sustainable Operations and Computers, 3, 2022, pp. 32–42, doi:10.1016/J.SUSOC.2021.09.004.
2. Shahrubudin N., Lee T.C., Ramlan R.: An overview on 3D printing technology: Technological, materials, and applications. Procedia Manufacturing, 35, 2019, pp. 1286–1296, doi:10.1016/J.PROMFG.2019.06.089.
3. Louvrier A., Marty P., Barrabé A., Euvrard E., Chatelain B., Weber E., Meyer C.: How useful is 3D printing in maxillofacial surgery?. Journal of stomatology, oral and maxillofacial surgery, 118, 2017, pp. 206–212, doi:10.1016/J.JORMAS.2017.07.002.
4. Fahem M.M., Ali N.H., Duddu J.R., Luther H.: Cold-Injection Molded Gentamicin-Impregnated Polymethyl Methacrylate Implants for Cranioplasty. Operative neurosurgery (Hagerstown, Md.), 21, 2021, pp. 248–257, doi:10.1093/ONS/OPAB257.
5. Fay C.D., Jeiranikhameneh A., Sayyar S., Talebian S., Nagle A., Cheng K., Fleming S., Mukherjee P., Wallace G.G.: Development of a customised 3D printer as a potential tool for direct printing of patient-specific facial prosthesis. International Journal of Advanced Manufacturing Technology, 120, 2022, pp. 7143–7155, doi:10.1007/S00170-022-09194-0/TABLES/2.
6. Szczygieł P.: Prototype of hand prosthesis components manufactured with biocompatible material using PolyJet Matrix technology. Mechanik, 95, 2022, pp. 50–54, doi:10.17814/MECHANIK.2022.7.10.
7. Duan X., Wang B., Yang L., Kadakia A.R.: Applications of 3D Printing Technology in Orthopedic Treatment. BioMed Research International, 2021, 2021, pp. 1–3, doi:10.1155/2021/9892456.
8. Mohapatra S., Kar R.K., Biswal P.K., Bindhani S.: Approaches of 3D printing in current drug delivery. Sensors International, 3, 2022, pp. 1–10, doi:10.1016/J.SINTL.2021.100146.
9. Wszoła M., Nitarska D., Cywoniuk P., Gomółka M., Klak M.: Stem Cells as a Source of Pancreatic Cells for Production of 3D Bioprinted Bionic Pancreas in the Treatment of Type 1 Diabetes. Cells, 10, 2021, pp. 1–23, doi:10.3390/CELLS10061544.
10. Szklanny A.A., Machour M., Redenski I., Chochola V., Goldfracht I., Kaplan B., Epshtein M., Simaan Yameen H., Merdler U., Feinberg A., et al.: 3D Bioprinting of Engineered Tissue Flaps with Hierarchical Vessel Networks (VesselNet) for Direct Host-To-Implant Perfusion. Advanced Materials, 33, 2021, pp. 1–19, doi:10.1002/ADMA.202102661.
11. Park J.M., Jeon J., Koak J.Y., Kim S.K., Heo S.J.: Dimensional accuracy and surface characteristics of 3D-printed dental casts. The Journal of prosthetic dentistry, 126, 2021, pp. 427–437, doi:10.1016/J.PROSDENT.2020.07.008.
12. Kitamori H., Sumida I., Tsujimoto T., Shimamoto H., Murakami S., Ohki M.: Evaluation of mouthpiece fixation devices for head and neck radiotherapy patients fabricated in PolyJet photopolymer by a 3D printer. Physica medica, 58, 2019, pp. 90–98, doi:10.1016/J.EJMP.2019.02.002.
13. Mustahsan V.M., Anugu A., Komatsu D.E., Kao I., Pentyala S.: Biocompatible Customized 3D Bone Scaffolds Treated with CRFP, an Osteogenic Peptide. Bioengineering (Basel, Switzerland) 2021, 8, doi:10.3390/BIOENGINEERING8120199.
14. Kozior T., Bochnia J., Gogolewski D., Zmarzły P., Rudnik M., Szot W., Szczygieł P., Musiałek M.: Analysis of Metrological Quality and Mechanical Properties of Models Manufactured with Photo-Curing PolyJet Matrix Technology for Medical Applications. Polymers, 14, 2022, pp. 1–18, doi:10.3390/POLYM14030408.
15. Rudnik M., Hanon M.M., Szot W., Beck K., Gogolewski D., Zmarzły P., Kozior T.: Tribological Properties of Medical Material (MED610) Used in 3D Printing PJM Technology. Tehnicki Vjesnik, 29, 2022, pp. 1100–1108, doi:10.17559/TV-20220111154304.
16. Bakowski H., Krzysiak Z.: Estimation of tribological properties of selected plastics materials manufactured by extrusion and 3d printing. Tribologia, 294, 2020, pp. 7–12, doi:10.5604/01.3001.0014.8330.
17. Niemczewska-Wójcik M.: Concept For A Research Methodology Of Surface Topography – Testing And Analysis Of Tribological Wear Traces. Tribologia, 302, 2022, pp. 31–38, doi:10.5604/01.3001.0016.1607.

18. Gogolewski D., Kozior T., Zmarzły P., Mathia T.G.: Morphology of models manufactured by slm technology and the ti6al4v titanium alloy designed for medical applications. Materials, 14, 2021, pp. 1–18, doi:10.3390/MA14216249.
19. Ryniewicz W., Bojko Ł., Ryniewicz A.M., Pihut M., Pałka P.: Tribological studies of layered biomaterials for prosthetic structures based on substructures made of digital technologies. Tribologia, 287, 2019, pp. 87–99, doi:10.5604/01.3001.0013.6566.
20. Piotrowska K., Madej M., Niemczewska-Wójcik M.: Properties of coatings used in biotribological systems. Engineering of Biomaterials, 2022, 2022, pp. 25–31, doi:10.34821/ENG.BIOMAT.164.2022.25-31.
21. Piotrowska K., Madej M., Ozimina D.: Assessment of the Functional Properties of 316L Steel Alloy Subjected to Ion Implantation Used in Biotribological Systems. Materials, 14, 2021, pp. 1–21, doi:10.3390/MA14195525.
22. Ozimina D., Piotrowska K., Madej M., Granek A.: The Influence of Ion Implantation on the Properties of Ti6Al4V Titanium Alloy in Biotribological Systems. Tribologia, 4, 2020, pp. 27–36, doi:10.5604/01.3001.0014.5895.
23. Stratasys: Biocompatible Clear MED610, 2018, (Available online) www.stratasys.com/siteassets/materials/materials-catalog/biocompatible/mds_pj_med610_0720a.pdf
24. EN ISO 10993-10:2013: Biological Evaluation of Medical Devices - Part 10: Tests for Irritation and Skin Sensitization, 2013.
25. EN ISO 10993-5:2009: Biological Evaluation of Medical Devices — Part 5: Tests for in Vitro Cytotoxicity, 2009.
26. EN ISO 10993-3:2014: Biological Evaluation of Medical Devices — Part 3: Tests for Genotoxicity, Carcinogenicity and Reproductive Toxicity, 2014.
27. EN ISO 10993-18:2009: Biological Evaluation of Medical Devices - Part 18: Chemical Characterization of Materials, 2009.
28. Stratasys: MSDS Clear Bio-Compatible MED610 Material Safety Data Sheet, 2011, (Available online) www.sys-uk.com/wp-content/uploads/2016/01/MSDS-Clear-Bio-Compatible-MED610-English-US-1.pdf
29. Stratasys: Support SUP705 Material Safety Data Sheet, 2021, (Available online) www.stratasys.co.in/siteassets/materials/materials-catalog/polyjet-materials/polyjet-support-materials/sds-06136_26sep21_british-english_eghs_support_sup705.pdf
30. Zmarzły P., Kozior T., Gogolewski D.: Dimensional and shape accuracy of foundry patterns fabricated through photo-curing. Tehnicki Vjesnik, 26, 2019, pp. 1576–1584, doi:10.17559/TV-20181109115954.
31. GEWA. DELRIN (POM) Technical Data (obtained at the request of the authors in paper form).
32. GEWA. NYLON 6.6 (PA) Technical Data (obtained at the request of the authors in paper form).